1.2

Surface Water and Energy Budgets for the Mississippi River Basin

Xia Feng*, Paul Houser*+
*Department of Climate Dynamics, George Mason University, Fairfax, VA
+Center for Research on Environment and Water, Calverton, MD

1. Introduction

The Second phase of the Global Soil Wetness Project (GSWP2) is an ongoing modeling activity of the Global Energy and Water Cycle Experiment (GEWEX) Global Land-Atmosphere System Study (GLASS) and the International Satellite Land-Surface Climatology Project (ISLSCP) (Dirmeyer et al. 1999). The global datasets of land surface fluxes, state variables, and related hydrologic quantities are generated from offline numerical experiments using a variety of land surface models. This study attempts to compare the surface water and energy budgets from baseline experiment model output using the Center for Ocean-Land-Atmosphere (COLA) Simplified Version of the Simple Biosphere Model (SSiB; Xue et al. 1991), Noah Land Surface Model (Noah; Ek et al. 2003) and Community Land Surface Model (CLM2-TOP; Bonan et al. 2002, hereafter CLM2) over the Mississippi River basin using the GSWP2 dataset.

2. Data and model

a. Research domain

The Mississippi River basin (Fig. 1) covers approximately 3.2 million km^2 and its agricultural economy profit is $100 billion per year (Goolsby et al. 1999). This area has many meteorological and hydrological datasets and was the focus region of the GEWEX Continental Scale International Project (Coughlan and Avissar 1996).

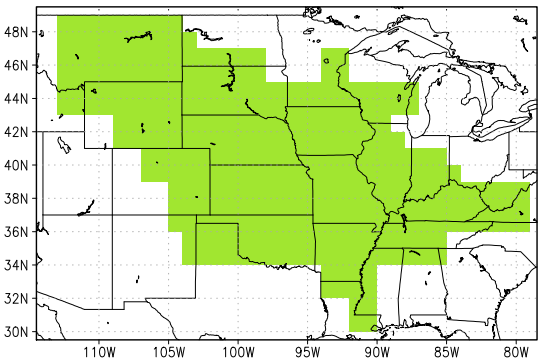

FIG. 1. The Mississippi River basin (green area).

* *Corresponding author address*: Xia Feng, 4041 Powder Street, Suite 302, Calverton, MD 20705; email: xfeng@gmu.edu

b. GSWP2 data

The water balance components, including precipitation, evaporation, runoff and water storage change as well as energy balance components, including short wave, net long wave radiations, latent heat and sensible heat and ground heat are available from the GSWP2 baseline model simulations. The GSWP2 model output covers the 10-year period from 1986 to 1995.

c. USGS surface stream flow data

The monthly Mississippi River stream flow data were obtained from the USGS website (http://water.usgs.gov.nwis), based on measurements made at the Vicksburg, Mississippi gage.

d. Precipitation

GSWP2 precipitation forcing is primarily based on a hybridization of National Centers for Environmental Prediction/Department of Energy (NCEP/DOE) reanalysis, the Global Precipitation Climatology Center (GPCC) gridded gauge analysis (Rudolf et al. 1994) and the Climate Research Unit (CRU) high resolution gauge measurements. When gauge density is low, Global Precipitation Climatology Project (GPCP) monthly product is blended in. We also use the 2.5×2.5 degree monthly global GPCP combined satellite and station precipitation (Adler 1994) and 0.25×0.25 degree daily U.S. Unified precipitation (Higgins 2000) for comparison with GSWP2 forcing precipitation product.

e. Model

Three land surface models used for the comparative study are listed in section 1.

3. Surface water

a. Surface water budget

The surface water balance equation is expressed as

$$\frac{\partial W}{\partial t} = P - E - R + U \qquad (1)$$

where W is the surface water (including soil moisture and snow water equivalent), P precipitation, E evaporation, R runoff including the surface and subsurface flow, U the miscellaneous term (such as change of surface liquid water storage and change in canopy interception storage).

b. Annual cycle

Figure 2 represents the annual cycle of monthly precipitation, evaporation and runoff for the Mississippi river basin during the period 1986-1995. Three GSWP2 land surface models utilize same precipitation forcing which is higher than GPCP and the Unified precipitation, but shows consistent seasonal variability (Fig. 2a). The monthly mean evaporation exhibits salient seasonal cycle with maximum in summer and minimum in spring and winter (Fig. 2b). Considerable evaporation occurs ($E >$30mm/month) after snowmelt, and attains a yearly maximum value of 100mm/month for CLM2 model on July. The SSiB and Noah models produce less evaporation than the CLM2 model which may be caused by the overly wet surface, convection and planetary boundary parameterizations. Peak discharge is associated with snowmelt during spring, with secondary contributions due to summertime rainstorms (Fig. 2c). Runoff is smaller in CLM2 which agrees very well with observations (Fig. 2c). By contrast, SSiB and Noah overestimate runoff. The change of surface water varies significantly among the three models during summer time (Fig. 2d).

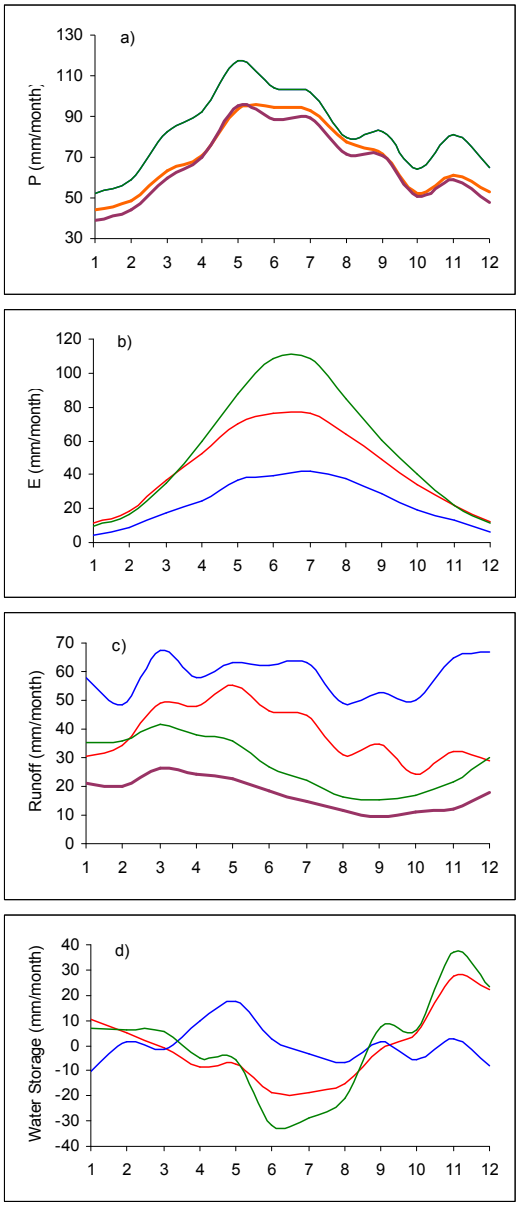

FIG. 2. The annual cycle of monthly mean a) precipitation, b) evaporation, c) runoff and d) change of water storage for SSiB (red), Noah (blue) and CLM2 (green) during 1986 to 1995. The observed GPCP (heavy orange) and Unified (heavy purple) precipitation in a), runoff gauge measurement (heavy purple) in c).

c. Interannual variability

Figure 3 shows a time series of annual precipitation, evaporation and runoff from all the models during the period 1986-1995. Dry periods are noticeable in 1988, 1992 and 1994 and wet periods in 1990 and 1993 (Fig. 3a). Evaporation shows slight interannual variability (Fig. 3b) but is consistent with the annual cycle of precipitation. It

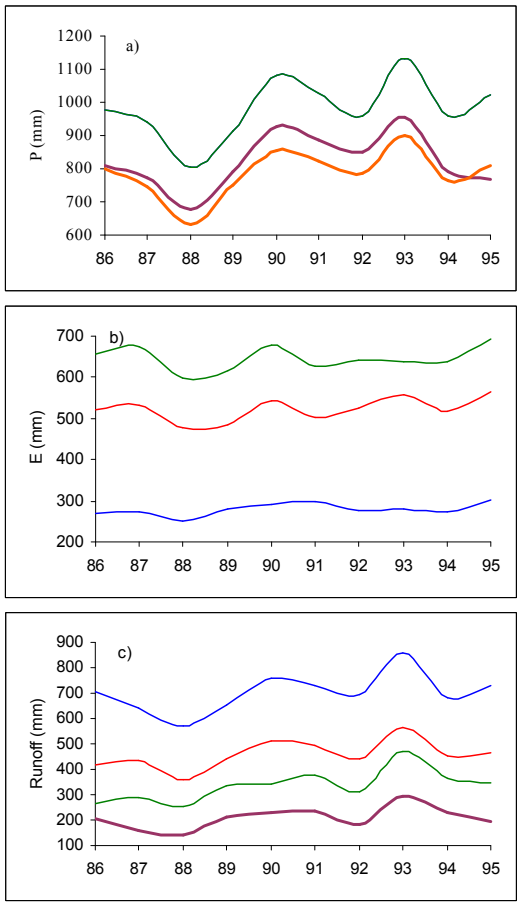

FIG.3. Annual a) precipitation, b) evaporation, and c) runoff for SSiB (red) Noah (blue) and CLM2 (green) during 1986 to 1995. The observed GPCP (heavy orange) and Unified (heavy purple) precipitation in a), runoff gauge (heavy purple) measurement in c).

is not surprising that small and large evaporation are associated with dry and wet year, respectively. CLM2 produces larger annual evaporation than Noah and SSiB; which is consistent with its seasonal variability. All three models overestimate the runoff (Fig. 3d). This is not surprising since the observation is surface streamflow, whereas the model includes the subsurface runoff in addition to the surface runoff. The 10-year mean $P-E$ is equal to R from three models (Table 1), which suggests that the long-term water cycle is balanced for the Mississippi river basin.

Table 1. Annual water budget from SSiB, Noah and CLM2 for Mississippi river basin (mmy^{-1}).

Model	P	E	P-E	Runoff
SSiB	992	527	465	465
Noah	992	283	709	709
CLM2	992	662	330	330

As mentioned before, the precipitation for all three models are the same. So we will mainly focus on the interannual variability of evaporation and runoff. Figure 4 shows time series ratio of JFM (January-February-March) and JJA (June-July-August) accumulated evaporation and total annual evaporation, respectively for three models for the Mississippi river basin. It is apparent that evaporation is less in winter than summer. Summer evaporation for individual year exceeds 40% of annual mean (Fig. 4b), highlighting the importance of summer evaporation. There is winter minimum and summer maximum evaporation occurring in 1993 summer, and a minimum in 1988 summer. Since evaporation in

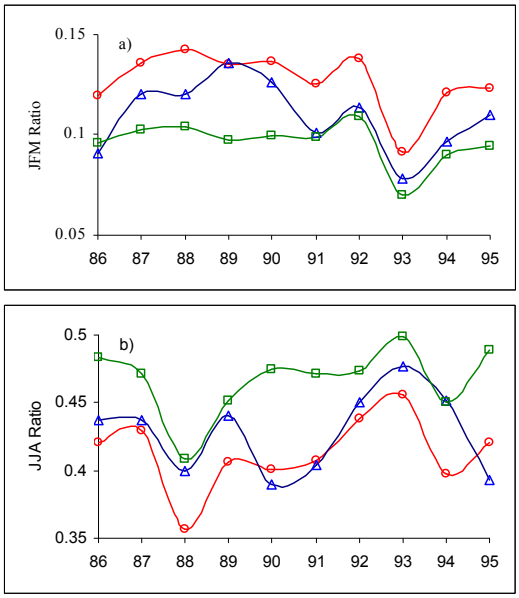

FIG. 4. Ratio of a) JFM and b) JJA evaporation to total evaporation for SSiB (red with circle), Noah (blue with triangle) and CLM2 (green with square) during 1986 to 1995.

CLM2 is larger than SSiB and Noah, as a consequence, the amount of seasonal evaporation is also large. However, CLM2 has a larger summer evaporation, and SSiB's maximum runoff occurred during the snow melt season (Fig. 5). JFM runoff exhibits three peaks occurring in 1988, 1991 and 1994. CLM2 is close to the observed runoff variation than SSiB and Noah. JJA runoff appears to have a 5-year cycle during 1986 to 1995; which is also associated with dry and wet years (Fig 3a). Note, JJA precipitation, evaporation and runoff (not shown) are similar to their corresponding annual values. This suggests that the interannual variation of JJA precipitation, evaporation and runoff contributes considerably to that of the annual values.

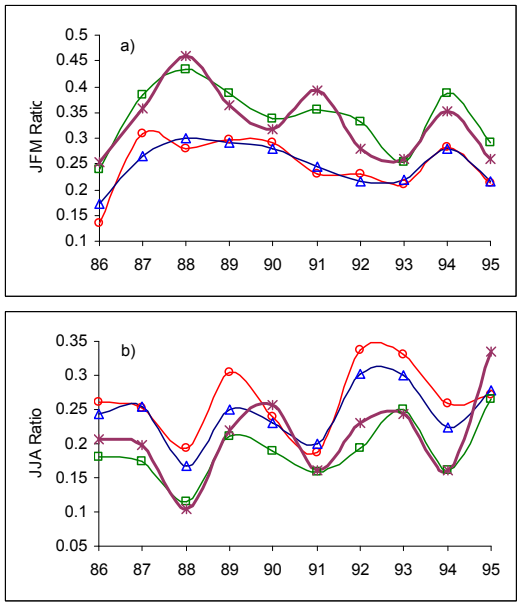

FIG.5. Same as in Fig. 4 for runoff. Gauge measurement is denoted by heavy purple.

The variations of the monthly anomalies in the surface hydrological cycle are shown in Fig. 6. The magnitude and variation for each model exhibit greater similarity than the corresponding annual mean values. There is a clear interannual signal in GSWP2 precipitation which is consistent with GPCP and Unified precipitation (Fig. 6a). Evaporation anomalies exhibit large discrepancies during the 1988 and 1989 summers, and the 1991 winter (Fig. 6b). The SSiB and CLM2 models show good agreement with each other. In particular, they show extreme years during 1988 and 1989 (less evaporation) and during 1992 and 1993 (strong evaporation), which are associated with strong ENSO events (discussed later). Runoff from three models show similar interannual variation, and the CLM2 model agrees well with the observation (Fig. 6c). However, the SSiB and Noah models overestimate the runoff interannual signal.

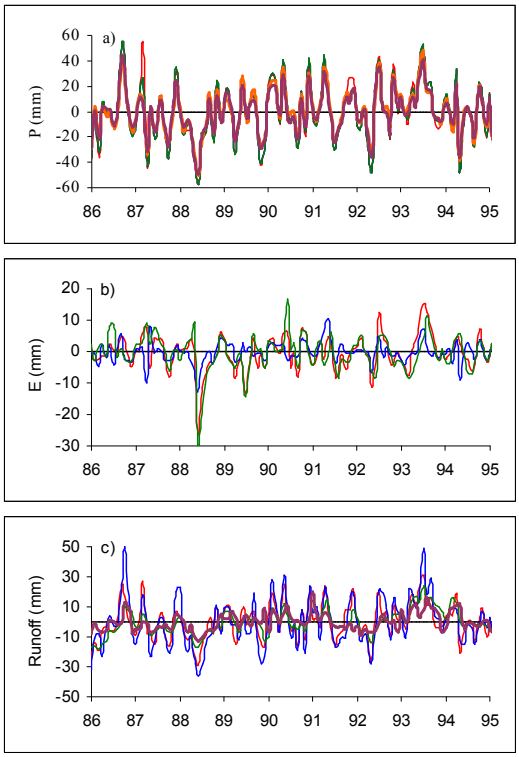

FIG. 6. Monthly anomaly of a) precipitation, b) evaporation and c) runoff for SSiB (red), Noah (blue) and CLM2 (green) during 1986 to 1995. The observed GPCP (heavy orange) and Unified (heavy purple) precipitation in a), runoff gauge measurement (heavy purple) in c).

d. Relationship with ENSO index

There are a total of eight ENSO events that occurred during 1986 to 1995 period (Table 2). How do these events influence the water cycle variability over the Mississippi River basin? What components of water cycle are closely related ENSO events? To address these questions, let's look at Fig. 7, which shows a JJA anomaly of precipitation, evaporation and runoff related to ENSO index. We are interested in summer water cycle variability, so we restrain the ENSO index during winter and spring. In addition, studies also suggest the ENSO signal is stronger during winter season. Precipitation shows consistency with the ENSO index during 1988, 1992 and 1993 (Fig. 7a). This phenomenon is only based on 10-years of data; it's hard to determine how ENSO influences precipitation. A long record of observation or model simulation is needed to investigate this relationship further. Evaporation from the three models exhibits strong consistency with ENSO events (Fig. 7b). Is this coincidence? This needs to be further studied using real observations. Runoff is also consistent with precipitation (Fig. 7c), and it only shows association with 4 ENSO events. Although the linkage between winter (December-January-February) precipitation, evaporation and runoff and ENSO index is not shown here, it is worthy know what they would look like.

Table 2. List of NINO 3.4 region index during 1986 to 1995.

Year	NINO 3.4 index	Season
1986		
1987	1.35	JFM
1988	-0.73	AMJ
1989	-1.46	JFM
1990		
1991	0.74	AMJ
1992	1.74	JFM
1993	1.06	AMJ
1994	1.14	OND
1995	0.73	JFM

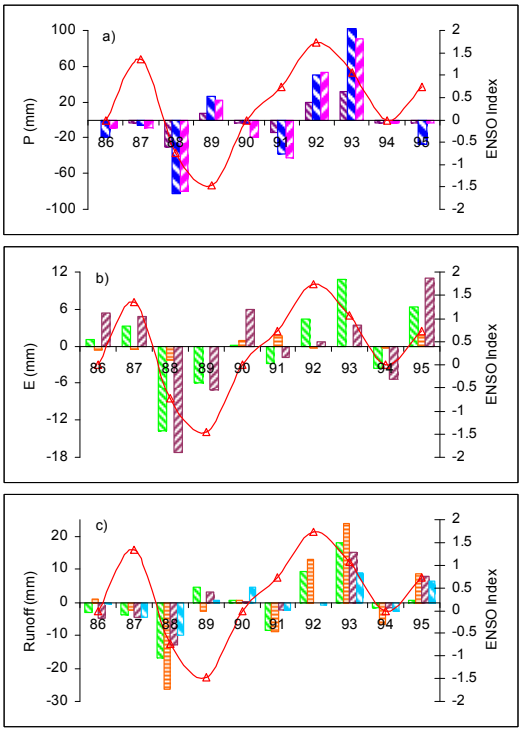

FIG. 7. Relationship of JJA anomaly of a) precipitation, b) evaporation and c) runoff for SSiB (green), Noah (orange) and CLM2 (purple) with ENSO index (red line) during 1986 to 1995. The observed GPCP (blue) and Unified (pink) precipitation in a), runoff gauge measurement (cyan) in c).

4. Surface energy

a. Surface energy budget

The surface energy equation is written as

$$0 = SW + LW - LH - SH - G + U \qquad (2)$$

Where SW and LW are the net shortwave and longwave radiations, respectively, LH the latent heat, SH the sensible heat, G the flux into the ground, and U the miscellaneous term such as snow melting and surface ground heat storage.

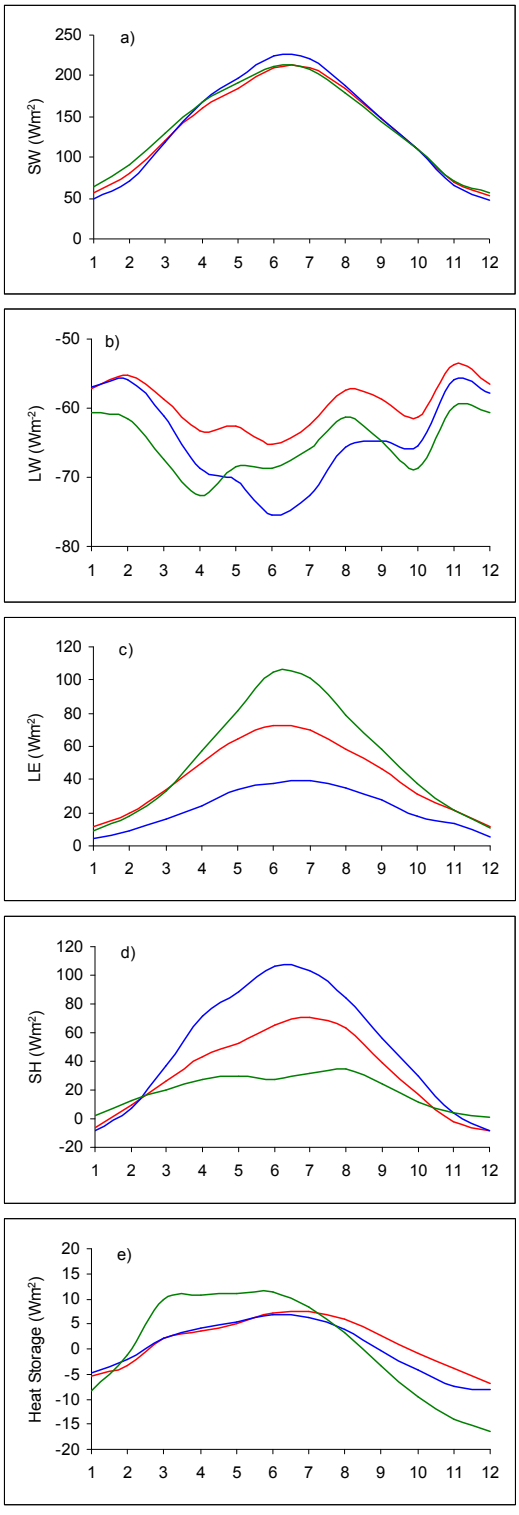

FIG. 8. Seasonal surface energy budgets from SSiB (red), Noah (blue) and CLM2 (green) for the Mississippi river basin: a) net surface short wave radiation, b) net surface longwave radiation, c) latent heat, d) sensible heat, and e) ground heat.

b. Comparison results

The seasonal energy balance is show in Fig. 8. Net shortwave radiation simulated from three models are in good agreement with each other (Fig. 8a). Net radiation between incoming solar radiation and outgoing longwave radiation (Fig. 8b) is partitioned into latent heat and sensible heat. All three models capture the seasonal variation of latent and sensible heat, with maximum occurring at summer, and a minimum in winter (Fig. 8c, d). There is strong latent heat variability (Fig. 9b). Roads et al. (2000) suggest

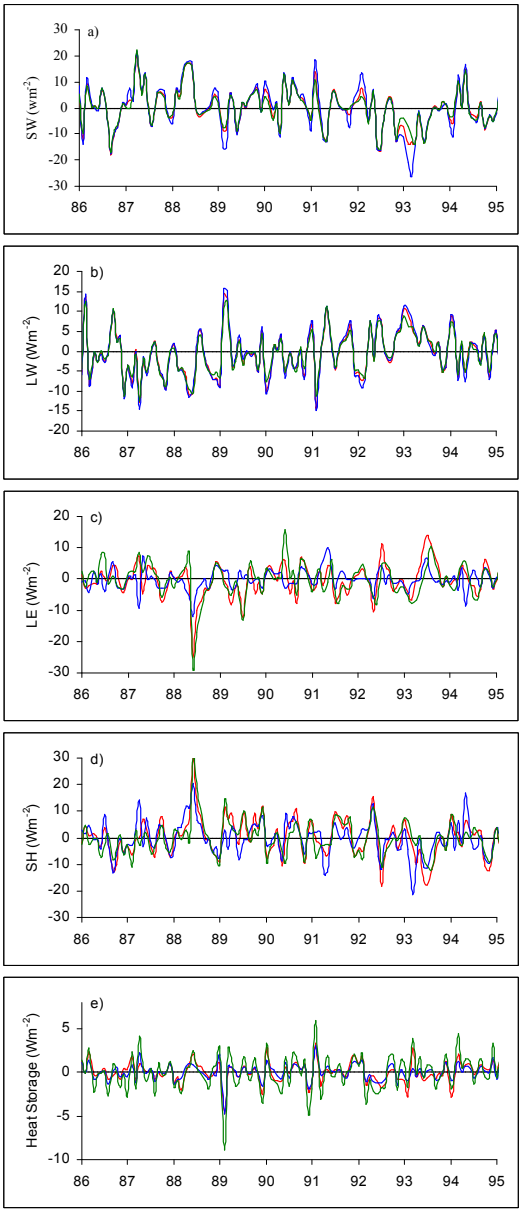

FIG. 9. Monthly anomaly of a) net surface short wave radiation, b) net surface longwave radiation, c) latent heat, d) sensible heat, and e) ground heat runoff for SSiB (red), Noah (blue) and CLM2 (green) during 1986 to 1995.

that the variations in cloudiness may contribute to this contrast. Latent heat and sensible heat both show a big spike at 1988 summer and 1993 summer, but with a negative correlation (Fig. 9c and d). The ground heat anomaly patterns are consistent among theses three models (Fig. 9e).

5. Summary

Similarities and differences among three land surface models in replicating the monthly, annual and interannual variability of the water cycle and energy budgets for the Mississippi River basin are presented and discussed in this study.

Seasonal and annual cycles of GSWP2 precipitation forcing are close to the GPCP and unified precipitation, although some underestimation occurs. The simulated evaporation exhibits a remarkable seasonal cycle; CLM2 generates larger evaporation than the SSiB and Noah models. Since all models use the same precipitation forcing, the resulting runoff from CLM is the smallest among the three models. However, it is closer to the observed runoff. In addition, summer evaporation accounts for more than 40% of overall annual mean. This ratio is larger than the corresponding precipitation and runoff. The monthly anomaly of precipitation, evaporation and runoff show a strong interannual signal, particularly in 1988 and 1993, which corresponds to the Mississippi River basin drought and flood events, respectively. Furthermore, the anomaly of latent heat and sensible heat also exhibit extreme interannual variability for these two years. The JJA anomaly of evaporation shows a close relationship with ENSO events, while precipitation and runoff only are associated with four of seven ENSO events.

In order to verify above conclusions, further analysis needs to focus on a comparison of the model simulated water budget and energy with the observed evaporation, net radiation, latent and sensible heat as well as other quantities.

References

Adler, R.F., G.J. Huffman, and P.R. Keehn, 1994: Global rain estimates from microwave-adjusted geosynchronous IR data. *Remote Sens. Rev*., **11**, 125-15.

Bonan, G.B., K.W. Oleson, M. Vertenstein, S. Levis, X. Zeng, Y. Dai, R.E. Dickinson, and Z.-L. Yang, 2002: The land surface climatology of the Community Land Model coupled to the NCAR Community Climate Model, *J. Climate*, **15**, 3123-3149.

Coughlan, M., and R. Advissar, 1996: The Global Energy and Water Cycle Experiment (GEWEX) Continental-Scale International Project (GCIP): An overview. *J. Geophs. Res.*, **101**(D3), 7139-7147.

Dirmeyer, P. A., A. J. Dolman, and N. Sato, 1999: The Global Soil Wetness Project: A pilot project for global land surface modeling and validation. *Bull. Amer. Meteor. Soc.*, **80**, 851-878.

Ek, M. B., K. E. Mitchell, Y. Lin, P. Grunmann, E. Rogers, G. Gayno, V. Koren, and J.D. Tarpley, Implementation of the upgraded noah land-surface model in the NCEP operational mesoscale Eta model, *J.Geophys, Res.*, **108** (D22), 8851, doi:10.1029/2002 JD003296, 2003.

Goolsby, D. A., and Coauthors, 1999: Flux and sources of nutrients in the Mississippi-Atchafalaya River basin. *Topic 3 report for the Integrated Assessment on Hypoxia in the Gulf of Mexico*. NOAA Coastal Ocean Office, Series No. 17, 130pp.

R. W. Higgins, W. Shi, E. Yarosh, R.Joyce, 2000: Improved United States Precipitation Quality Control System and Analysis. *NCEP/Climate Prediction Center ATLAS No. 7*, U. S. DEPARTMENT OF COMMERCE, National Oceanic and Atmospheric Administration, National Weather Service.

Roads, John and Alan Betts, 2000: NCEP-NCAR and ECMWF reanalysis surface water and energy budgets for the Mississippi River basin. *J. Hydrometeor.*,**1**, 88-94.